Misshapen decreases integrin levels to promote epithelial motility and planar polarity in *Drosophila*

Lindsay Lewellyn,[1] Maureen Cetera,[2] and Sally Horne-Badovinac[1,2]

[1]Department of Molecular Genetics and Cell Biology, and [2]Committee on Development, Regeneration and Stem Cell Biology, The University of Chicago, Chicago, IL 60637

Complex organ shapes arise from the coordinate actions of individual cells. The *Drosophila* egg chamber is an organ-like structure that lengthens along its anterior–posterior axis as it grows. This morphogenesis depends on an unusual form of planar polarity in the organ's outer epithelial layer, the follicle cells. Interestingly, this epithelium also undergoes a directed migration that causes the egg chamber to rotate around its anterior–posterior axis. However, the functional relationship between planar polarity and migration in this tissue is unknown. We have previously reported that mutations in the Misshapen kinase disrupt follicle cell planar polarity. Here we show that Misshapen's primary role in this system is to promote individual cell motility. Misshapen decreases integrin levels at the basal surface, which may facilitate detachment of each cell's trailing edge. These data provide mechanistic insight into Misshapen's conserved role in cell migration and suggest that follicle cell planar polarity may be an emergent property of individual cell migratory behaviors within the epithelium.

Introduction

During development, changes in organ shape require the precise coordination of individual cell behaviors across tissues. The *Drosophila* egg chamber provides a highly tractable system to investigate the cellular control of organ morphogenesis. Egg chambers are simple, multicellular structures within fly ovaries that will each give rise to a single egg. They consist of a central germ cell cluster surrounded by an epithelial layer of follicle cells. The apical epithelial surface faces the germ cells, whereas the basal surface contacts a basement membrane (BM) extracellular matrix (ECM; Fig. 1, A and B). Though initially spherical, each egg chamber lengthens along its anterior–posterior (AP) axis as it grows. The elongation depends on an unusual form of planar polarity at the basal epithelial surface, in which linear bundles of actin filaments and fibril-like structures in the BM both align perpendicular to the AP axis (Gutzeit, 1990; Gutzeit et al., 1991). The resulting circumferential arrangement of structural molecules, which is first evident at the onset of elongation, is thought to act as a "molecular corselet" that directionally biases egg chamber growth (Gutzeit et al., 1991; He et al., 2010; Haigo and Bilder, 2011). Follicle cell planar polarity is independent of the Frizzled/Strabismus and Fat/Dachsous planar cell polarity pathways (Viktorinová et al., 2009). Instead, this system largely relies on cell–BM interactions, as mutations that block these processes disrupt planar polarity and produce round eggs (Bateman et al., 2001; Frydman and Spradling, 2001; Conder et al., 2007).

New insight has come from the recent discovery that egg chamber elongation is also linked to an unexpected epithelial migration. Coincident with planar polarization of the epithelium, the basal follicle cell surfaces migrate on the inside of the BM, such that the migration path is oriented perpendicular to the AP axis. This process causes the entire egg chamber to rotate within the BM, which remains largely stationary. The current model is that follicle cell migration creates the fibril-like structures in the BM, which contribute to the constrictive corselet (Haigo and Bilder, 2011). This migration is unusual, in that the follicle cells form a continuous epithelium with no leading edge. It is therefore possible that the planar polarity in this tissue coordinately aligns the cells' front–rear axes to set the direction for collective movement. However, the functional relationship between follicle cell planar polarity and tissue migration is unknown.

We have previously reported that mutations in the Ste20 kinase Misshapen (Msn) disrupt follicle cell planar polarity (Horne-Badovinac et al., 2012). Here we show that Msn functions autonomously within each follicle cell to promote its motility.

Correspondence to Sally Horne-Badovinac: shorne@uchicago.edu

Abbreviations used in this paper: AP, anterior–posterior; BM, basement membrane; JNK, c-Jun N-terminal kinase; Msn, Misshapen.

The Rockefeller University Press $30.00
J. Cell Biol. Vol. 200 No. 6 721–729
www.jcb.org/cgi/doi/10.1083/jcb.201209129

Msn decreases integrin levels at the basal epithelial surface, which appears to facilitate the detachment of each cell's trailing edge. These findings provide mechanistic insight into Msn's conserved role in cell migration. They also suggest that follicle cell planar polarity may, in fact, be an emergent property of individual cell migratory behaviors within the epithelium.

Results and discussion

To investigate Msn's role in egg chamber elongation, we depleted the protein from the follicle cells by RNAi using *TubP-Gal4* (Zhu and Stein, 2004), and confirmed that this condition produces round eggs (Fig. S1 A). Although control epithelia migrated normally, Msn-depleted epithelia remained completely stationary (Fig. 1, C and D; and Video 1). Importantly, *msn-RNAi* egg chambers also become significantly rounder than controls, concurrent with the onset of follicle cell migration at stage 6 (Fig. S1 B). These data suggest that a key role for Msn during egg chamber elongation is to promote follicle cell migration.

We have previously reported that loss of Msn in large clones leads to a global defect in follicle cell planar polarity during migration stages (Horne-Badovinac et al., 2012). We therefore hypothesized that the motility defect exhibited by *msn-RNAi* epithelia might occur at the tissue level, reflecting an inability of the follicle cells to coordinately orient their front–rear axes. Surprisingly, however, visualization of migration dynamics in mosaic epithelia revealed that Msn is autonomously required for individual cell motility. Although large *msn* mutant clones block egg chamber rotation, the wild-type cells still show what appears to be a very slow, directed migration. In contrast, the mutant cells are completely still (Fig. 1 E and Video 2). To gain further insight into this defect, we produced small clones of 2–3 cells expressing *msn-RNAi*. Here, the wild-type cells migrate relatively normally (0.42 µm/min), and the egg chamber rotates as in controls (Fig. 1 F and Video 3). Interestingly, the Msn-depleted cells now also migrate, but at a much slower rate (0.14 µm/min), likely due to incomplete knockdown. Unlike normal follicle cell migration, where individual cells rarely change neighbors (Haigo and Bilder, 2011), the wild-type cells easily slide past the slower moving clone, showing that variations in migration speed across the tissue can induce unexpected changes in cell–cell contacts. These data show that, although large *msn* clones can inhibit the migration of the entire epithelium, Msn primarily functions cell-autonomously to promote individual follicle cell motility.

During these mosaic analyses, we observed a novel phenotype that further highlights Msn's cell-autonomous function. When a clone is confined to one of the egg chamber's poles, the wild-type cells at the clone boundary break contact with their mutant neighbors and invade the egg chamber's interior, sometimes bisecting the germ cell cluster (Fig. 2 A). Under these conditions, planar polarization of the basal actin filaments is maintained (Fig. 2 B), and the egg chambers elongate (Fig. 2, A–C). Unlike genetic perturbations that cause mutant follicle cells to invade the germ cells (Goode and Perrimon, 1997; Bilder et al., 2000; Lu and Bilder, 2005), the wild-type cells maintain their cuboidal morphology and contact with a BM (Fig. S1 C). Depletion of Msn specifically in the anterior follicle cells using *C306-Gal4* also causes invasion (Fig. 2 C).

We have observed how this surprising phenotype develops by performing live imaging on an egg chamber with a small anterior clone. At the start of the experiment, the wild-type cells at the clone boundary had just begun to invade (Fig. 2 D, 0 min). Imaging at the basal surface of the same egg chamber revealed that the noninvading wild-type cells migrated normally, and the egg chamber rotated (Fig. 2 E and Video 4). Returning to the transverse plane, the invading wild-type cells had continued to move toward one another through the germ cell cluster (Fig. 2 D, 90 min). These data suggest that the wild-type cells undergo a wound healing–like response to exclude the nonmigratory mutant cells from the epithelium and preserve the ability of the remaining cells to migrate (schematized in Fig. 2 F). Thus, the invasion phenotype appears to be an extreme example of the cell-autonomous nature of the *msn* migration defect that also induces a novel behavior in the wild-type cells.

Previous work had demonstrated that clones of immotile follicle cells can be carried along the migration path by their wild-type neighbors (Haigo and Bilder, 2011). Why then do *msn*-null mutant clones remain stationary? Msn homologues in other organisms have been implicated in regulating integrin-based adhesion (Becker et al., 2000; Poinat et al., 2002; Wright et al., 2003; Martynovsky et al., 2012). Therefore, we next investigated whether Msn performs a similar function in this context. The predominant integrin heterodimer expressed by the migrating follicle cells contains the α-PS1 and β-PS subunits (Delon and Brown, 2009). Immunofluorescence studies of mosaic epithelia revealed a cell-autonomous increase in both subunits at the basal surface of *msn* cells (Fig. 3 A). In contrast, expression of an activated, membrane-tethered form of Msn (Myr-Msn; Kaneko et al., 2011) decreased integrin levels (Fig. 3 B). In some tissues, Msn activates the c-Jun N-terminal kinase (JNK) signaling pathway (Su et al., 1998; Paricio et al., 1999); however, loss of the JNK kinase Basket in follicle cell clones does not affect integrin levels (Fig. S2 A). These results indicate that Msn functions in a JNK-independent manner to decrease integrins at the basal follicle cell surface.

During their migration, the follicle cells create fibril-like structures in the BM (Haigo and Bilder, 2011), a phenomenon best observed with a GFP protein trap of one of the type IV collagen subunits, encoded by the *viking* gene (Vkg-GFP, Fig. 3 C; Buszczak et al., 2007). Consistent with the migration defect, *msn-RNAi* causes a severe disruption in the formation of BM fibrils. However, an even more striking defect is seen in *msn* mosaic epithelia. Here the Vkg-GFP contacting mutant cells becomes tightly associated with basal cell edges. This phenotype can also be seen to a lesser extent in the *msn-RNAi* condition. This cell-autonomous deformation of the BM suggests that the additional integrins at the basal surface may participate in active focal adhesions that increase BM contact and reduce cell movement.

If increased integrin levels produce the *msn* migration defect, reducing integrins in the *msn-RNAi* background should restore cell motility. By depleting Msn with a weaker follicle cell driver, *traffic jam-Gal4* (*tj-Gal4*), we found that 46% (6/13) of *msn-RNAi* epithelia now undergo very slow migration, providing

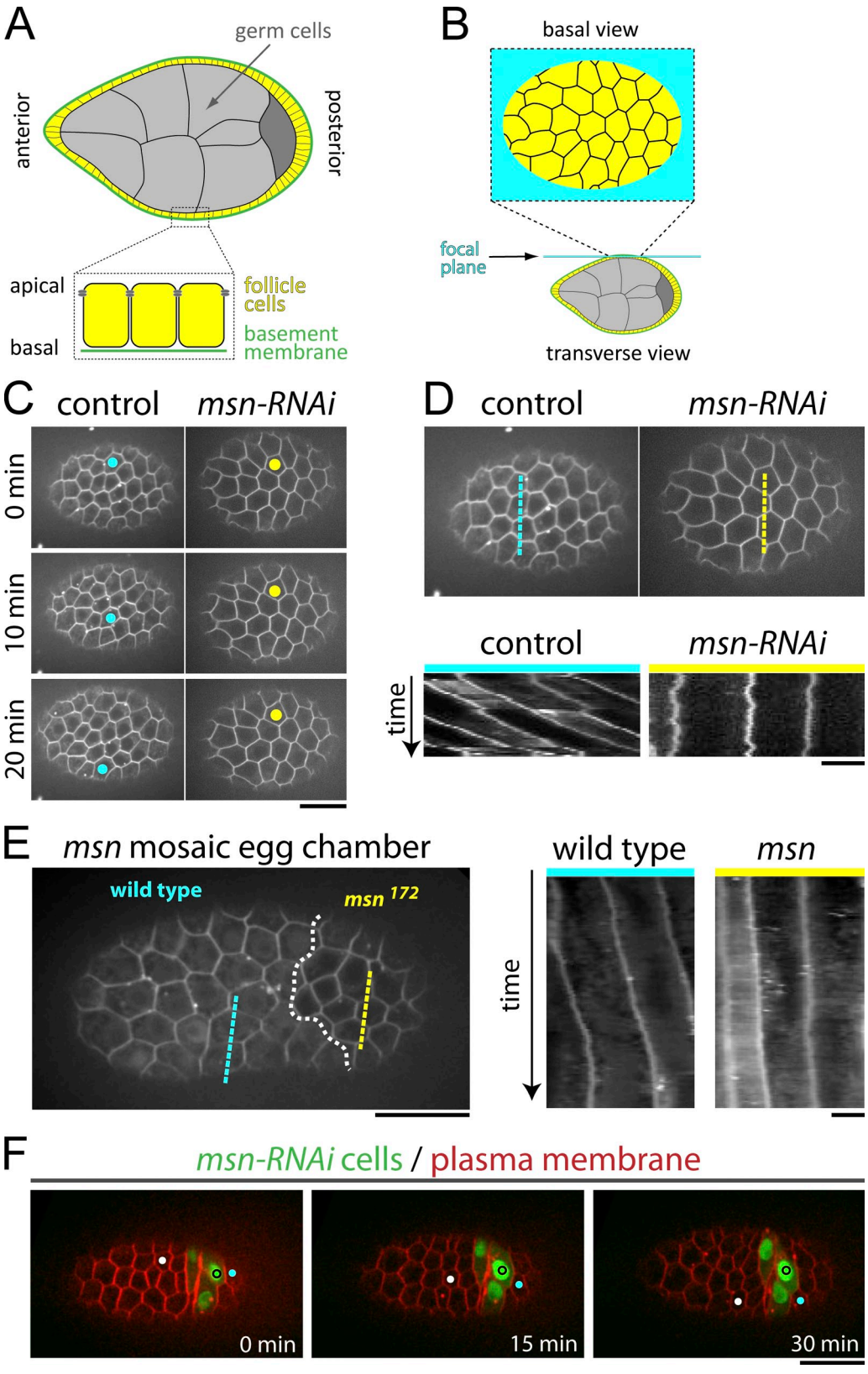

Figure 1. **Msn functions cell-autonomously to promote follicle cell migration.** (A) Overview of egg chamber structure. (B) Schematic for visualization of follicle cell migration. (C and D) *msn-RNAi* epithelia ($n = 15$) show migratory defects compared with control epithelia ($n = 19$). All imaging was performed on stage 6–7 egg chambers. (C) Stills from a time lapse (Video 1) of stage 6 control and *msn-RNAi* epithelia, in which a single follicle cell is monitored over time (blue and yellow dots). (D) Maximum intensity kymograph drawn through control or *msn-RNAi* follicle cells (dotted lines). (E) Maximum intensity kymograph drawn through wild-type (blue) and msn^{172} (yellow) cells in a mosaic epithelium (Video 2). (F) Stills from a time lapse (Video 3) of an *msn-RNAi* flipout clone (GFP). Bars: (C, E, and F; egg chamber images) 20 µm; (D and E; kymographs) 5 µm.

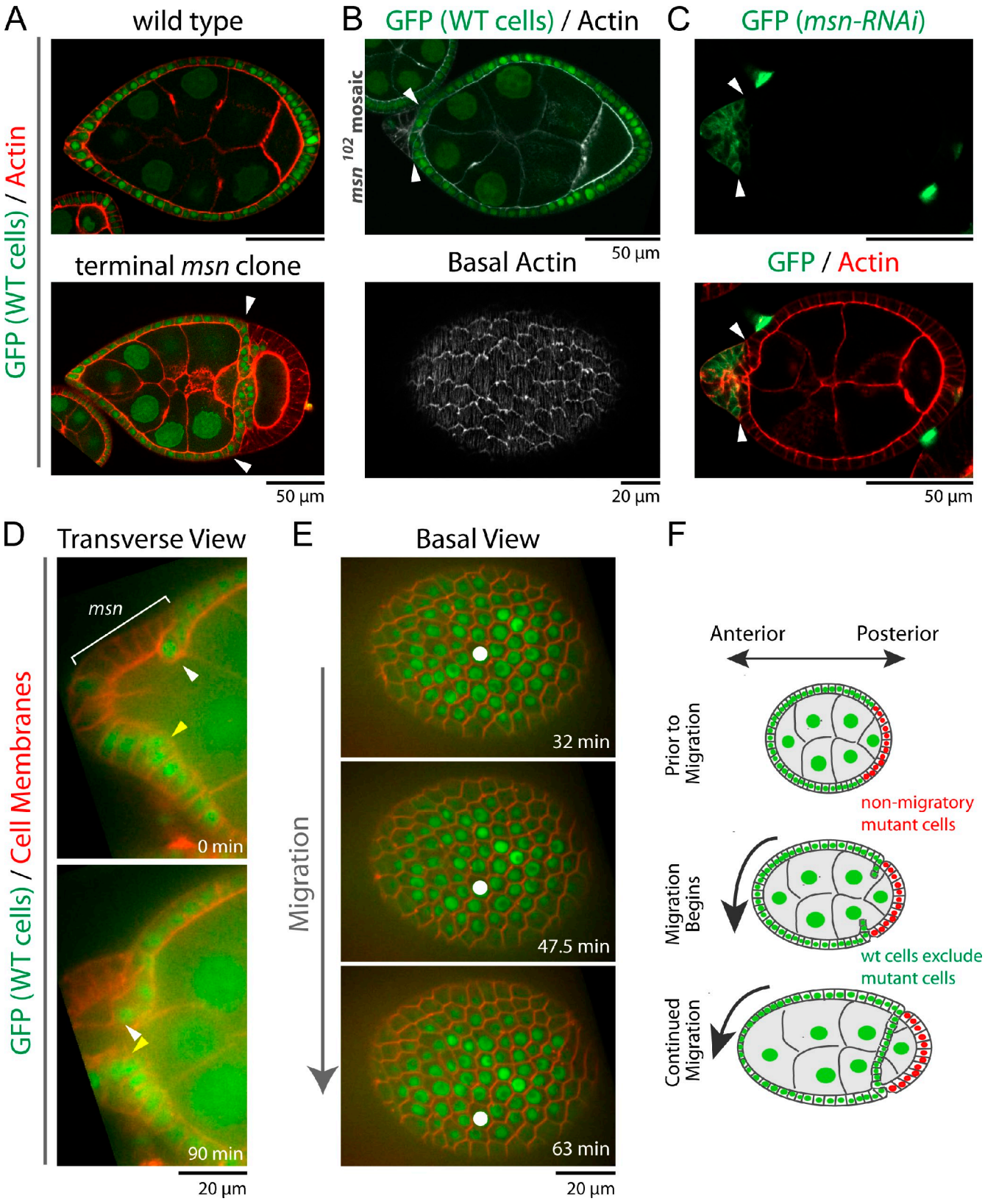

Figure 2. **Terminal *msn* clones induce a novel invasion phenotype.** (A) Transverse section showing that a posterior terminal *msn* clone causes neighboring wild-type cells (GFP) to invade the germ cells (arrowheads). (B) An invasion event (arrowheads) does not disrupt planar polarization of the basal actin filaments. (C) Expressing *msn-RNAi* exclusively in the anterior follicle cells (GFP) also causes invasion (arrowheads). (D) Initial and final frames of a time lapse (Video 4) taken of an msn^{172} mosaic egg chamber with an anterior terminal clone (bracket). Wild-type cells (GFP) adjacent to the mutant clone invade the germ cells (arrowheads). (E) Stills from the same time lapse acquired at the basal surface show that the noninvading wild-type cells continue to migrate. Bars are as indicated in the figure. (F) Model for how the invasion phenotype develops over time.

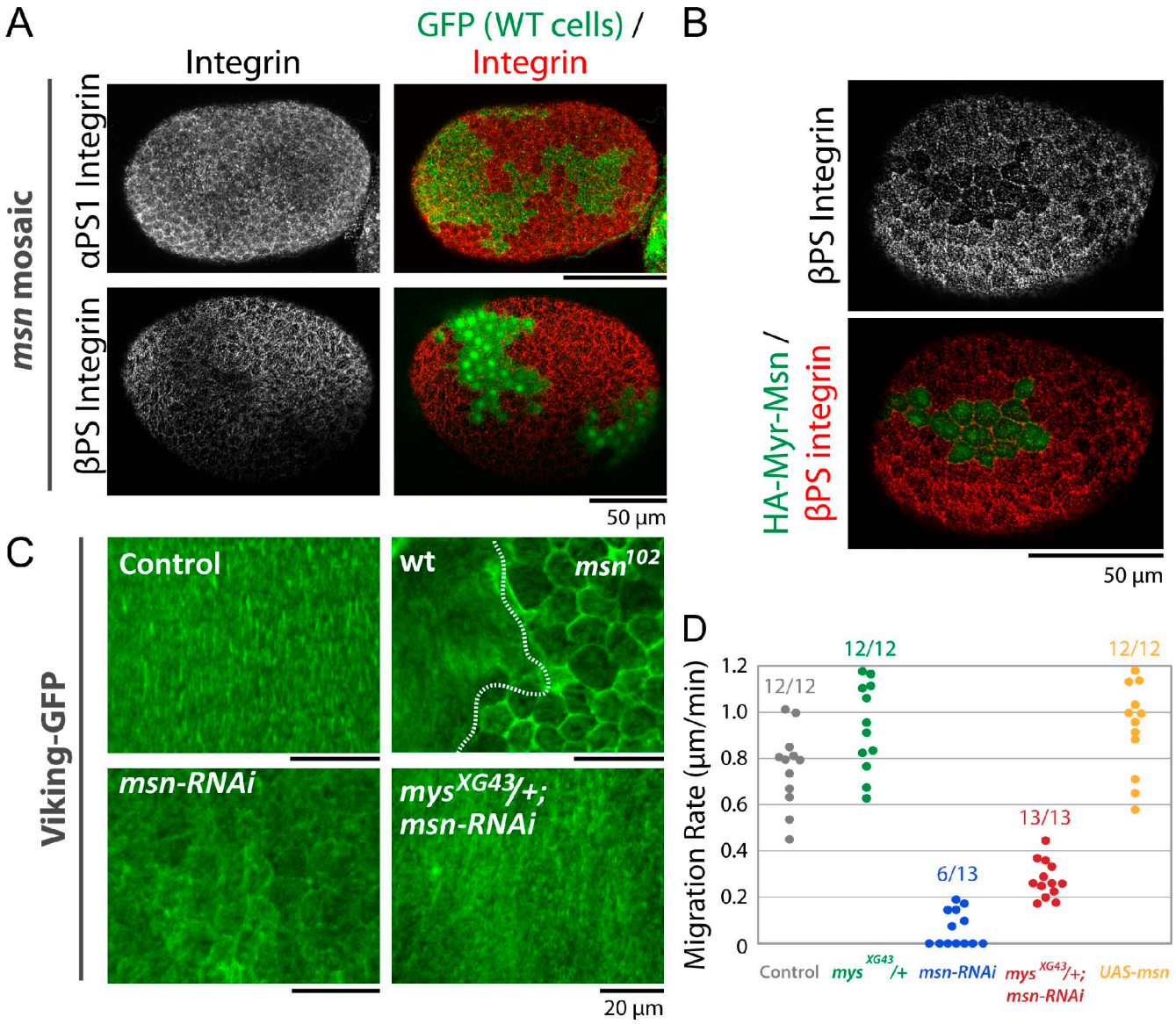

Figure 3. **Msn reduces integrin-based adhesion.** (A) Basal views of *msn* mosaic epithelia stained with antibodies against α-PS1 (maximum projection) or β-PS show increased integrin levels at the basal surfaces of *msn* cells. GFP marks wild-type cells. (B) A clone of cells expressing an activated form of Msn (green) shows reduced integrins at the basal surface. (C) Maximum projection of Vkg-GFP in the BM. Loss of Msn disrupts BM structure in a cell-autonomous manner, and BM structure is restored by introducing one copy of a loss-of-function *β-PS* mutation (*mys^{XG43}/+; msn-RNAi*). Bars are as indicated in the figure. (D) Removing one copy of *β-PS* also rescues the defect in follicle cell migration seen in *msn-RNAi*, whereas removing one copy of *β-PS* alone or overexpressing Msn (UAS-Msn) increases the migration rate. Graph shows migration rates of individual stage 6–7 egg chambers for each condition. Numbers indicate fraction of egg chambers that showed follicle cell migration. The data shown are from a single representative experiment out of two repeats. Each experimental condition involves egg chambers dissected from >10 female flies, imaged over multiple days.

a sensitized condition for phenotypic rescue (Fig. 3 D). We then introduced one copy of a null β-PS integrin mutation, *myospheroid^{XG43}* (*mys^{XG43}*), into this background. Strikingly, 100% (13/13) of these epithelia are motile (Fig. 3 D). Reducing integrin levels in *msn-RNAi* epithelia also rescues follicle cell planar polarity and Vkg-GFP polarization (Figs. S2 B and 3 C), suggesting that increased integrin-based adhesion may produce these phenotypes as well.

We were surprised to find, however, that reducing integrin levels alone increases the average rate of follicle cell migration (Fig. 3 D; control, 0.76 ± 0.17 µm/min; *mys^{XG43}*/+, 0.93 ± 0.19 µm/min). This observation is consistent with previous reports showing that changes in ECM adhesion strength can affect migration speed (Palecek et al., 1997; Gupton and Waterman-Storer, 2006), but it also raises the possibility that the rescue we observed of the *msn-RNAi* migration phenotype is simply an additive effect of combining faster migrating and slower migrating states. Motivated by this unexpected result, we overexpressed Msn in the follicle cells and found that this condition also increases epithelial migration rates (Fig. 3 D; 0.95 ± 0.20 µm/min). All together, our results support a model in which Msn decreases the integrin-based adhesion of the follicle cells to the BM.

To further investigate the mechanism by which Msn regulates cell motility, we used a fluorescent protein trap in the *msn* gene (Msn-YFP) to reveal this protein's localization. During follicle cell migration, Msn-YFP shows a clear planar polarized

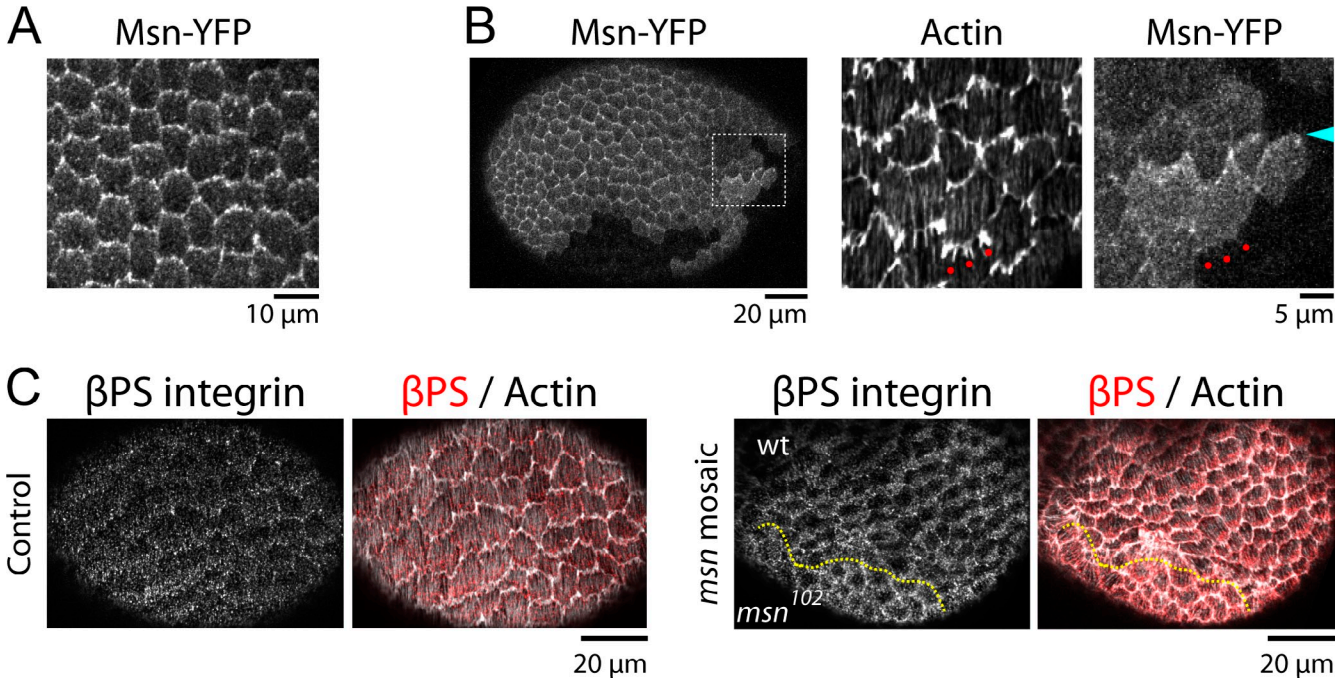

Figure 4. **Msn is enriched at the trailing edge of each migrating cell.** (A) Msn-YFP shows a planar polarized distribution at the basal surface. (B) Follicle cell clones expressing Msn-YFP show that this protein is enriched at the back (blue arrowhead) of each migrating cell. Dots indicate filopodial protrusions at the front of the cell. (C) Basal views of control and *msn* mosaic epithelia stained with antibodies against β-PS. There is a slight enrichment of integrins at the leading edge of each follicle cell, which is disrupted in a clone of *msn* cells. All images are maximum intensity projections of the basal surface.

distribution at the basal epithelial surface (Fig. 4 A). Previous reports showed that the follicle cells also extend filopodia from their basal surfaces in a planar polarized pattern (Gutzeit, 1991). Live imaging has revealed that these structures mark the leading edge of each migrating cell (unpublished data). Using mitotic recombination to create isolated clones of Msn-YFP cells, we found that the heightened Msn localization always occurs on the opposite side of the cell from the filopodia, showing that Msn is enriched at each cell's trailing edge (Fig. 4 B). β-PS integrin shows a complementary localization pattern, being slightly enriched at the front of each migrating cell (Fig. 4 C). This polarization is lost in clones of *msn* cells (Fig. 4 C). Together, these data suggest that Msn may reduce integrin-based adhesion at the cell's trailing edge.

To test this idea, we returned to the small *msn-RNAi* clones that maintain the ability to migrate, albeit at a slower rate (Fig. 1 F). Interestingly, these cells are often elongated with tail-like extensions, a phenotype never observed in wild-type clones (Fig. 5 A). Live imaging confirmed that the tails correspond to the cell's trailing edge (Fig. 5 B and Video 5), and that they can eventually retract as the cell moves forward (Fig. 5 C and Video 6). Interestingly, we have also observed prominent foci of the focal adhesion protein Talin/Rhea within the small *msn-RNAi* clones, which are often enriched in the tail (Fig. 5 D). These data support an increased requirement for Msn at the cell's trailing edge.

Here we have shown that Msn's primary function during egg chamber elongation is to promote follicle cell motility. This finding is consistent with previous work establishing Msn and its homologues as pro-migratory kinases (Poinat et al., 2002; Collins et al., 2006; Chapman et al., 2008; Cobreros-Reguera et al., 2010; Teulière et al., 2011; Martynovsky et al., 2012). However, it is important to note that the mechanistic role that individual family members play in cell movement can vary with cell type. In the follicle cells, our data are consistent with a model in which Msn reduces integrin-based adhesion to the BM. Msn homologues in mice and *Caenorhabditis elegans* directly bind the β-integrin tail, suggesting that Msn could play a proximal role in focal adhesion turnover (Poinat et al., 2002). Msn's enrichment at the basal follicle cell surface and its known association with the focal adhesion component Dreadlocks/NCK also support such a mechanism (Ruan et al., 1999; Buday et al., 2002). However, it is possible that Msn controls focal adhesion dynamics indirectly through modulation of the actin cytoskeleton (Fu et al., 1999; Ruan et al., 2002; Baumgartner et al., 2006; Köppen et al., 2006; Shakir et al., 2006). Our data further suggest a greater requirement for Msn at the cell's trailing edge. This aspect of Msn's function may also be conserved, as the *C. elegans* homologue MIG-15 limits cell-protrusive activity at the back of migrating growth cones (Teulière et al., 2011). Thus, we propose that Msn regulates follicle cell motility, at least in part, by inducing cell detachment at the trailing edge.

This work also sheds light on the mechanisms by which epithelial cells migrate at the tissue level. Consistent with in vitro studies (Palecek et al., 1997; Gupton and Waterman-Storer, 2006), we have shown that increasing or decreasing follicle cell–BM adhesion strength can alter epithelial migration rates in vivo. Importantly, our studies of *msn* mosaic epithelia demonstrate the robust nature of this tissue's migratory behavior. Because Msn-deficient cells adhere more tightly to the BM, small clones cannot be carried along the migration path by their wild-type neighbors. Consequently, wild-type cells at the clone boundary modify

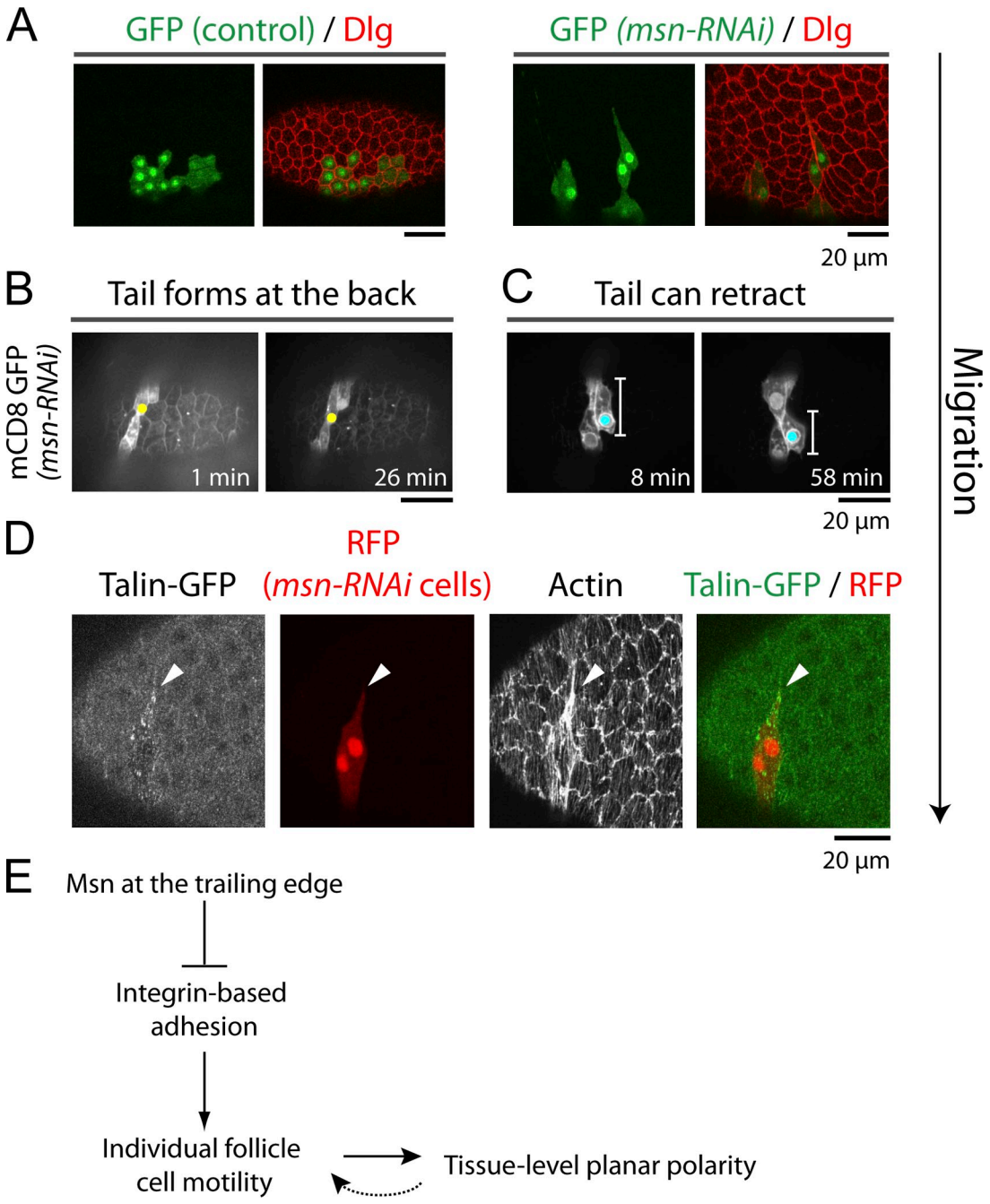

Figure 5. **Msn appears to promote detachment of the cell's trailing edge.** (A) Control and *msn-RNAi* flipout clones (GFP) show that Msn depletion causes cell stretching, often forming a "tail" at one end. (B and C) Stills from two time-lapse movies of egg chambers with clones of cells expressing *msn-RNAi* and mCD8-GFP (Videos 5 and 6), which show that the "tails" form at the trailing edge of the migrating *msn-RNAi* cells (B), and can retract as the cells move forward (C). (D) Maximum projection of the basal surface in an egg chamber expressing Talin-GFP with *msn-RNAi* flipout clones (RFP). The migration direction for all panels is down (arrow). (E) Schematic for Msn's role in follicle cell migration and planar polarity.

cell–cell adhesion to either increase neighbor exchange or fully exclude the *msn* clone, thus preserving tissue-level migration and the morphogenetic program for egg chamber elongation.

We have previously shown that Msn is required for planar polarization of the follicle cell epithelium (Horne-Badovinac et al., 2012). Our current finding that Msn functions autonomously within each follicle cell to promote its motility now raises the intriguing possibility that tissue-level planar polarity may, in fact, arise from individual cell migratory behavior. Recent studies have shown that forces exerted by epithelial morphogenesis or by tension from neighboring tissues can align the Frizzled/Stabismus planar cell polarity system (Aigouy et al., 2010; Olguín et al., 2011; Lee et al., 2012). We propose that follicle cell planar polarity has a similar morphogenetic basis (Fig. 5 E). Our studies of *msn* mosaic epithelia show a positive correlation between tissue-level migration and planar polarity that is dependent on clone size. Similarly, loss of the atypical cadherin Fat2 from less than 50% of the follicle cells has no effect

on planar polarity, whereas larger clones cause global disruptions (Viktorinová et al., 2009, 2011). We envision that this binary phenotype could also result from the success or failure of tissue migration. If enough wild-type cells are present to drive bulk epithelial movement, this would be sufficient to align the basal actin filaments and BM fibrils across the entire tissue. In this way, individual cell migratory behaviors can be translated into the tissue-level polarity required for organ morphogenesis.

Materials and methods

Drosophila genetics

Full genotypes for each experiment are in Table S1. Most crosses that involved clone generation were performed at 25°C, with the exception of RNAi experimental crosses that were raised at 18°C and shifted to higher temperatures as indicated in Table S2. All *msn* follicle cell clones were produced using *FRT80B*, and *e22c-Gal4* to drive expression of the FLP recombinase in the follicle stem cells. *bsk*$^{Df(2L)flp147E}$ clones were generated using *FRT40A* and the FLP recombinase under the control of a heat shock promoter. For flipout clones, *UAS* lines were crossed to flies containing the FLP recombinase under a heat shock promoter as well as the *act5c>>Gal4, UAS-GFP* (*or UAS-RFP*) flipout cassette. Most lines were obtained from the Bloomington *Drosophila* Stock Center (Bloomington, IN), with exceptions listed here. *UAS-msn-RNAi* (v101517 KK) is from the Vienna *Drosophila* RNAi Center (Vienna, Austria). *tj-Gal4* (104055) and *msn-YFP* (115454) are from the *Drosophila* Genetic Resource Center (Kyoto Institute of Technology, Kyoto, Japan; Rees et al., 2011). *vkg-GFP* (CC00791) is from the Carnegie Protein Trap Library (Buszczak et al., 2007). *UAS-HA-myr-msn* is from Kaneko et al. (2011). *UAS-msn* is from Su et al. (2000). *UAS-mCD8-GFP* is from Pfeiffer et al. (2010). *msn*$^{P23\text{-}5}$*, FRT80/TM3* is from Horne-Badovinac et al. (2012). The genetic lesion in *mys*^{XG43}*, FRT101/FM6* is described in Jannuzi et al. (2002). *Talin(rhea)-GFP/TM6b* is from Venken et al. (2011). *msn*^{102} *and msn*^{172} are available from the Bloomington *Drosophila* Stock Center, but were first described in Treisman et al. (1997). *w*^{1118} served as a wild-type control. For experiments involving heat shock, females were placed on yeast in an EchoTherm programmable incubator (Torrey Pines Scientific), heat shocked twice daily for 2 d, and then dissected 2–3 d later. Each heat shock consisted of a 1-h period at 37°C, with a 1-h recovery at 25°C, followed by a second hour at 37°C.

Live imaging

A highly detailed protocol for egg chamber live imaging can be found in Prasad et al. (2007). For this study, female flies were fed yeast to increase egg production. Ovaries were then dissected from the females in live imaging media, which consists of Schneider's *Drosophila* medium (Invitrogen) supplemented with 200 µg/ml insulin (Sigma-Aldrich), 15% (vol/vol) fetal bovine serum, and 0.6× streptomycin/penicillin (Invitrogen) at pH 6.95–7.0. Ovaries were removed from the female by using one set of forceps to submerge her in the media and the other set to pull on the posterior-most part of the abdomen, revealing the pair of ovaries. Individual ovarioles were then isolated from the muscle sheath by gently pulling on the germarium with forceps. Egg chambers were transferred into live imaging media with 0.4% NuSieve GTG low melt agarose (Lonza) and 6 µM FM4-64 (Invitrogen) to label cell membranes, and mounted in an aluminum slide (76 cm × 26 cm) containing a circular hole (12-cm diameter) with a coverslip attached to the bottom using melted parafilm. The agarose was allowed to solidify for ∼10 min, and then egg chambers were imaged with a 63×/1.4 NA oil-immersion objective on a microscope (Axiovert 200M; Carl Zeiss) equipped with a spinning disk unit (model CSU-10; Yokogawa Corporation of America) and illuminated with 50-mW 473-nm (GFP) and 25-mW 561-nm (mCherry) diode pump solid-state lasers. Images were acquired with an EM-CCD camera (Cascade 512B; Photometrics) controlled by MetaMorph software (Molecular Devices).

Immunohistochemistry and microscopy

Ovaries were dissected in S2 medium and fixed for 15 min in PBS + 0.1% Triton + 4% EM-grade formaldehyde (Polysciences). Antibody stains were performed in PBS + 0.1–0.3% Triton + 0.1% BSA. Alexa Fluor 488– or 555–conjugated secondary antibodies were used (1:200; Invitrogen). Rhodamine (1:200; Sigma-Aldrich) or Alexa Fluor 647 Phalloidin (1:50; Invitrogen) was used to label F-actin. Samples were mounted in SlowFade Antifade (Invitrogen) and imaged at room temperature using a 40×/1.3 NA EC Plan-NeoFluar oil objective on a laser-scanning confocal microscope (LSM510; Carl Zeiss) controlled by the LSM acquisition software. Maximum intensity projections were generated using ImageJ (National Institutes of Health) as indicated, and images were compiled using Photoshop CS4 (Adobe). Commercial antibodies include: anti-HA (1:200; rabbit; Rockland), and anti-Myc (1:200; mouse; Cell Signaling Technology). The following antibodies were obtained from the Developmental Studies Hybridoma Bank, developed under the auspices of the National Institute of Child Health and Human Development and maintained by The University of Iowa, Department of Biology (Iowa City, IA): Dlg (4F3; 1:10 supernatant), α-PS1 (DK.1A4; 1:50 concentrate), and β-PS (COMPARE6G11; 1:10 supernatant). Anti-laminin (rabbit, 1:50) was a generous gift from Lisa Fessler (UCLA, Los Angeles, CA).

Online supplemental material

Fig. S1 shows examples of the *msn* round egg phenotype and characterizes the effect of *msn-RNAi* on egg chamber elongation between stages 5 and 10. It also shows an example of *msn* mosaic egg chamber displaying the invasion phenotype, which has been stained for laminin. Fig. S2 shows that defects in JNK signaling do not affect integrin levels, and that reducing integrin levels rescues the defect in basal actin organization in *msn-RNAi* egg chambers. Supplemental videos show examples of egg chambers described in Fig. 1 C (Video 1), Fig. 1 E (Video 2), Fig. 1 F (Video 3), Fig. 2, D and E (Video 4), Fig. 5 B (Video 5), and Fig. 5 C (Video 6). Table S1 lists experimental genotypes used in each figure panel. Table S2 lists details for the temperatures at which the flies were maintained. Online supplemental material is available at http://www.jcb.org/cgi/content/full/jcb.201209129/DC1. Additional data are available in the JCB DataViewer at http://dx.doi.org/10.1083/jcb.201209129.dv.

Hugo Bellen, Lisa Fessler, Barret Pfeiffer, and Lan Xu generously provided reagents. We are also grateful to Julie Canman, Lisa Gallegos, Kirstin Sherrard, and members of the Horne-Badovinac laboratory for insightful comments on the manuscript; to Darcy McCoy for technical assistance; and to Nick Badovinac for illustrations.

Lindsay Lewellyn was supported by a Postdoctoral Fellowship (PF-12-135-01-CSM) from the American Cancer Society and an award from the American Heart Association. This work was further supported by grants from the Edward Mallinckrodt, Jr. Foundation and National Institutes of Health (R01 GM094276) to Sally Horne-Badovinac.

Submitted: 24 September 2012
Accepted: 19 February 2013

References

Aigouy, B., R. Farhadifar, D.B. Staple, A. Sagner, J.C. Röper, F. Jülicher, and S. Eaton. 2010. Cell flow reorients the axis of planar polarity in the wing epithelium of *Drosophila*. *Cell*. 142:773–786. http://dx.doi.org/10.1016/j.cell.2010.07.042

Bateman, J., R.S. Reddy, H. Saito, and D. Van Vactor. 2001. The receptor tyrosine phosphatase Dlar and integrins organize actin filaments in the *Drosophila* follicular epithelium. *Curr. Biol.* 11:1317–1327. http://dx.doi.org/10.1016/S0960-9822(01)00420-1

Baumgartner, M., A.L. Sillman, E.M. Blackwood, J. Srivastava, N. Madson, J.W. Schilling, J.H. Wright, and D.L. Barber. 2006. The Nck-interacting kinase phosphorylates ERM proteins for formation of lamellipodium by growth factors. *Proc. Natl. Acad. Sci. USA*. 103:13391–13396. http://dx.doi.org/10.1073/pnas.0605950103

Becker, E., U. Huynh-Do, S. Holland, T. Pawson, T.O. Daniel, and E.Y. Skolnik. 2000. Nck-interacting Ste20 kinase couples Eph receptors to c-Jun N-terminal kinase and integrin activation. *Mol. Cell. Biol.* 20:1537–1545. http://dx.doi.org/10.1128/MCB.20.5.1537-1545.2000

Bilder, D., M. Li, and N. Perrimon. 2000. Cooperative regulation of cell polarity and growth by *Drosophila* tumor suppressors. *Science*. 289:113–116. http://dx.doi.org/10.1126/science.289.5476.113

Buday, L., L. Wunderlich, and P. Tamás. 2002. The Nck family of adapter proteins: regulators of actin cytoskeleton. *Cell. Signal.* 14:723–731. http://dx.doi.org/10.1016/S0898-6568(02)00027-X

Buszczak, M., S. Paterno, D. Lighthouse, J. Bachman, J. Planck, S. Owen, A.D. Skora, T.G. Nystul, B. Ohlstein, A. Allen, et al. 2007. The carnegie protein trap library: a versatile tool for *Drosophila* developmental studies. *Genetics*. 175:1505–1531. http://dx.doi.org/10.1534/genetics.106.065961

Chapman, J.O., H. Li, and E.A. Lundquist. 2008. The MIG-15 NIK kinase acts cell-autonomously in neuroblast polarization and migration in *C. elegans*. *Dev. Biol.* 324:245–257. http://dx.doi.org/10.1016/j.ydbio.2008.09.014

Cobreros-Reguera, L., A. Fernández-Miñán, C.H. Fernández-Espartero, H. López-Schier, A. González-Reyes, and M.D. Martín-Bermudo. 2010. The Ste20 kinase misshapen is essential for the invasive behaviour of ovarian epithelial cells in *Drosophila*. *EMBO Rep.* 11:943–949. http://dx.doi.org/10.1038/embor.2010.156

Collins, C.S., J. Hong, L. Sapinoso, Y. Zhou, Z. Liu, K. Micklash, P.G. Schultz, and G.M. Hampton. 2006. A small interfering RNA screen for modulators of tumor cell motility identifies MAP4K4 as a promigratory kinase. *Proc. Natl. Acad. Sci. USA*. 103:3775–3780. http://dx.doi.org/10.1073/pnas.0600040103

Conder, R., H. Yu, B. Zahedi, and N. Harden. 2007. The serine/threonine kinase dPak is required for polarized assembly of F-actin bundles and apical-basal polarity in the *Drosophila* follicular epithelium. *Dev. Biol.* 305:470–482. http://dx.doi.org/10.1016/j.ydbio.2007.02.034

Delon, I., and N.H. Brown. 2009. The integrin adhesion complex changes its composition and function during morphogenesis of an epithelium. *J. Cell Sci.* 122:4363–4374. http://dx.doi.org/10.1242/jcs.055996

Frydman, H.M., and A.C. Spradling. 2001. The receptor-like tyrosine phosphatase lar is required for epithelial planar polarity and for axis determination within *Drosophila* ovarian follicles. *Development*. 128:3209–3220.

Fu, C.A., M. Shen, B.C. Huang, J. Lasaga, D.G. Payan, and Y. Luo. 1999. TNIK, a novel member of the germinal center kinase family that activates the c-Jun N-terminal kinase pathway and regulates the cytoskeleton. *J. Biol. Chem.* 274:30729–30737. http://dx.doi.org/10.1074/jbc.274.43.30729

Goode, S., and N. Perrimon. 1997. Inhibition of patterned cell shape change and cell invasion by Discs large during *Drosophila* oogenesis. *Genes Dev.* 11:2532–2544. http://dx.doi.org/10.1101/gad.11.19.2532

Gupton, S.L., and C.M. Waterman-Storer. 2006. Spatiotemporal feedback between actomyosin and focal-adhesion systems optimizes rapid cell migration. *Cell*. 125:1361–1374. http://dx.doi.org/10.1016/j.cell.2006.05.029

Gutzeit, H.O. 1990. The microfilament pattern in the somatic follicle cells of midvitellogenic ovarian follicles of *Drosophila*. *Eur. J. Cell Biol.* 53:349–356.

Gutzeit, H.O. 1991. Organization and in vitro activity of microfilament bundles associated with the basement membrane of *Drosophila* follicles. *Acta Histochem. Suppl.* 41:201–210.

Gutzeit, H.O., W. Eberhardt, and E. Gratwohl. 1991. Laminin and basement membrane-associated microfilaments in wild-type and mutant *Drosophila* ovarian follicles. *J. Cell Sci.* 100:781–788.

Haigo, S.L., and D. Bilder. 2011. Global tissue revolutions in a morphogenetic movement controlling elongation. *Science*. 331:1071–1074. http://dx.doi.org/10.1126/science.1199424

He, L., X. Wang, H.L. Tang, and D.J. Montell. 2010. Tissue elongation requires oscillating contractions of a basal actomyosin network. *Nat. Cell Biol.* 12:1133–1142. http://dx.doi.org/10.1038/ncb2124

Horne-Badovinac, S., J. Hill, G. Gerlach II, W. Menegas, and D. Bilder. 2012. A screen for round egg mutants in *Drosophila* identifies tricornered, furry, and misshapen as regulators of egg chamber elongation. *G3 (Bethesda).* 2:371–378.

Jannuzi, A.L., T.A. Bunch, M.C. Brabant, S.W. Miller, L. Mukai, M. Zavortink, and D.L. Brower. 2002. Disruption of C-terminal cytoplasmic domain of betaPS integrin subunit has dominant negative properties in developing *Drosophila*. *Mol. Biol. Cell*. 13:1352–1365. http://dx.doi.org/10.1091/mbc.01-08-0429

Kaneko, S., X. Chen, P. Lu, X. Yao, T.G. Wright, M. Rajurkar, K. Kariya, J. Mao, Y.T. Ip, and L. Xu. 2011. Smad inhibition by the Ste20 kinase Misshapen. *Proc. Natl. Acad. Sci. USA*. 108:11127–11132. http://dx.doi.org/10.1073/pnas.1104128108

Köppen, M., B.G. Fernández, L. Carvalho, A. Jacinto, and C.P. Heisenberg. 2006. Coordinated cell-shape changes control epithelial movement in zebrafish and *Drosophila*. *Development*. 133:2671–2681. http://dx.doi.org/10.1242/dev.02439

Lee, J., A. Andreeva, C.W. Sipe, L. Liu, A. Cheng, and X. Lu. 2012. PTK7 regulates myosin II activity to orient planar polarity in the mammalian auditory epithelium. *Curr. Biol.* 22:956–966. http://dx.doi.org/10.1016/j.cub.2012.03.068

Lu, H., and D. Bilder. 2005. Endocytic control of epithelial polarity and proliferation in *Drosophila*. *Nat. Cell Biol.* 7:1232–1239. http://dx.doi.org/10.1038/ncb1324

Martynovsky, M., M.C. Wong, D.T. Byrd, J. Kimble, and J.E. Schwarzbauer. 2012. mig-38, a novel gene that regulates distal tip cell turning during gonadogenesis in *C. elegans* hermaphrodites. *Dev. Biol.* 368:404–414. http://dx.doi.org/10.1016/j.ydbio.2012.06.011

Olguín, P., A. Glavic, and M. Mlodzik. 2011. Intertissue mechanical stress affects Frizzled-mediated planar cell polarity in the *Drosophila* notum epidermis. *Curr. Biol.* 21:236–242. http://dx.doi.org/10.1016/j.cub.2011.01.001

Palecek, S.P., J.C. Loftus, M.H. Ginsberg, D.A. Lauffenburger, and A.F. Horwitz. 1997. Integrin-ligand binding properties govern cell migration speed through cell-substratum adhesiveness. *Nature*. 385:537–540. http://dx.doi.org/10.1038/385537a0

Paricio, N., F. Feiguin, M. Boutros, S. Eaton, and M. Mlodzik. 1999. The *Drosophila* STE20-like kinase misshapen is required downstream of the Frizzled receptor in planar polarity signaling. *EMBO J.* 18:4669–4678. http://dx.doi.org/10.1093/emboj/18.17.4669

Pfeiffer, B.D., T.T. Ngo, K.L. Hibbard, C. Murphy, A. Jenett, J.W. Truman, and G.M. Rubin. 2010. Refinement of tools for targeted gene expression in *Drosophila*. *Genetics*. 186:735–755. http://dx.doi.org/10.1534/genetics.110.119917

Poinat, P., A. De Arcangelis, S. Sookhareea, X. Zhu, E.M. Hedgecock, M. Labouesse, and E. Georges-Labouesse. 2002. A conserved interaction between beta1 integrin/PAT-3 and Nck-interacting kinase/MIG-15 that mediates commissural axon navigation in *C. elegans*. *Curr. Biol.* 12:622–631. http://dx.doi.org/10.1016/S0960-9822(02)00764-9

Prasad, M., A.C. Jang, M. Starz-Gaiano, M. Melani, and D.J. Montell. 2007. A protocol for culturing *Drosophila melanogaster* stage 9 egg chambers for live imaging. *Nat. Protoc.* 2:2467–2473. http://dx.doi.org/10.1038/nprot.2007.363

Rees, J.S., N. Lowe, I.M. Armean, J. Roote, G. Johnson, E. Drummond, H. Spriggs, E. Ryder, S. Russell, D. St Johnston, and K.S. Lilley. 2011. In vivo analysis of proteomes and interactomes using Parallel Affinity Capture (iPAC) coupled to mass spectrometry. *Mol. Cell. Proteomics*. 10:M110.002386.

Ruan, W., H. Long, D.H. Vuong, and Y. Rao. 2002. Bifocal is a downstream target of the Ste20-like serine/threonine kinase misshapen in regulating photoreceptor growth cone targeting in *Drosophila*. *Neuron*. 36:831–842. http://dx.doi.org/10.1016/S0896-6273(02)01027-9

Ruan, W., P. Pang, and Y. Rao. 1999. The SH2/SH3 adaptor protein dock interacts with the Ste20-like kinase misshapen in controlling growth cone motility. *Neuron*. 24:595–605. http://dx.doi.org/10.1016/S0896-6273(00)81115-0

Shakir, M.A., J.S. Gill, and E.A. Lundquist. 2006. Interactions of UNC-34 Enabled with Rac GTPases and the NIK kinase MIG-15 in *Caenorhabditis elegans* axon pathfinding and neuronal migration. *Genetics*. 172:893–913. http://dx.doi.org/10.1534/genetics.105.046359

Su, Y.C., J.E. Treisman, and E.Y. Skolnik. 1998. The *Drosophila* Ste20-related kinase misshapen is required for embryonic dorsal closure and acts through a JNK MAPK module on an evolutionarily conserved signaling pathway. *Genes Dev.* 12:2371–2380. http://dx.doi.org/10.1101/gad.12.15.2371

Su, Y.C., C. Maurel-Zaffran, J.E. Treisman, and E.Y. Skolnik. 2000. The Ste20 kinase misshapen regulates both photoreceptor axon targeting and dorsal closure, acting downstream of distinct signals. *Mol. Cell. Biol.* 20:4736–4744. http://dx.doi.org/10.1128/MCB.20.13.4736-4744.2000

Teulière, J., C. Gally, G. Garriga, M. Labouesse, and E. Georges-Labouesse. 2011. MIG-15 and ERM-1 promote growth cone directional migration in parallel to UNC-116 and WVE-1. *Development*. 138:4475–4485. http://dx.doi.org/10.1242/dev.061952

Treisman, J.E., N. Ito, and G.M. Rubin. 1997. misshapen encodes a protein kinase involved in cell shape control in *Drosophila*. *Gene*. 186:119–125. http://dx.doi.org/10.1016/S0378-1119(96)00694-4

Venken, K.J., K.L. Schulze, N.A. Haelterman, H. Pan, Y. He, M. Evans-Holm, J.W. Carlson, R.W. Levis, A.C. Spradling, R.A. Hoskins, and H.J. Bellen. 2011. MiMIC: a highly versatile transposon insertion resource for engineering *Drosophila melanogaster* genes. *Nat. Methods*. 8:737–743. http://dx.doi.org/10.1038/nmeth.1662

Viktorinová, I., T. König, K. Schlichting, and C. Dahmann. 2009. The cadherin Fat2 is required for planar cell polarity in the *Drosophila* ovary. *Development*. 136:4123–4132. http://dx.doi.org/10.1242/dev.039099

Viktorinová, I., L.M. Pismen, B. Aigouy, and C. Dahmann. 2011. Modelling planar polarity of epithelia: the role of signal relay in collective cell polarization. *J. R. Soc. Interface*. 8:1059–1063. http://dx.doi.org/10.1098/rsif.2011.0117

Wright, J.H., X. Wang, G. Manning, B.J. LaMere, P. Le, S. Zhu, D. Khatry, P.M. Flanagan, S.D. Buckley, D.B. Whyte, et al. 2003. The STE20 kinase HGK is broadly expressed in human tumor cells and can modulate cellular transformation, invasion, and adhesion. *Mol. Cell. Biol.* 23:2068–2082. http://dx.doi.org/10.1128/MCB.23.6.2068-2082.2003

Zhu, X., and D. Stein. 2004. RNAi-mediated inhibition of gene function in the follicle cell layer of the *Drosophila* ovary. *Genesis*. 40:101–108. http://dx.doi.org/10.1002/gene.20070